Biomedical Research and Therapy 2026, 13(05):8558-8572

Open Access Full Text Article

Original Research

Localized subcutaneous injection of human umbilical cord derived mesenchymal stem cells attenuates psoriasis-like inflammation in an imiquimod-induced mouse model

Dao Thu Thi-Hong[1,3], Pham Phuc Van[1,3], Vu Ngoc Bich[1,2,3,*]

ABSTRACT

Abstract: Psoriasis is a chronic immune-mediated skin disorder driven by dysregulation of the IL-23/IL-17 axis. Human umbilical cord–derived mesenchymal stem cells (hUC-MSCs) possess immunomodulatory and anti-inflammatory properties, making them a potential therapeutic candidate for psoriasis treatment. In this study, we evaluated the therapeutic effects of localized subcutaneous administration of hUC-MSCs in an imiquimod (IMQ)-induced psoriasis-like mouse model. **Methods**: BALB/c mice received daily topical IMQ for six consecutive days. A single dose of hUC-MSCs (2.5×10^6 cells) was administered subcutaneously at lesional sites on day 2. Treatment with hUC-MSCs significantly attenuated clinical severity, as evidenced by reduced erythema, scaling, and skin thickness, along with decreased epidermal hyperplasia and inflammatory infiltration. **Results**: Analysis demonstrated a reduction in IL-17A and IL-23 expression in lesional skin at day 6 following hUC-MSC treatment. Consistently, quantitative PCR revealed downregulation of multiple psoriasis-associated inflammatory genes, with more pronounced suppression observed for downstream mediators such as *Tnf* and *Ccl20*, while upstream cytokines within the IL-23/IL-17 axis (Il17a, Il23) showed more moderate changes. By day 12, gene expression levels declined across all groups, reflecting the self-resolving nature of the IMQ-induced model. **Conclusion**: Overall, these findings demonstrate that localized subcutaneous administration of hUC-MSCs attenuates psoriasis-like inflammation and accelerates lesion resolution in an IMQ-induced mouse model, potentially through modulation of key proinflammatory cytokines. Further studies are required to evaluate long-term efficacy and to elucidate the underlying mechanisms of action.

Key words: hUC-MSCs, psoriasis, IL-23/IL-17 axis, immunomodulation, subcutaneous injection, cytokines

[1]*Stem Cell Institute, University of Science Ho Chi Minh City, Viet Nam*

[2]*Faculty of Biology - Biotechnology, University of Science, Ho Chi Minh City, Viet Nam*

[3]*Vietnam National University Ho Chi Minh City, Viet Nam*

Correspondence

Vu Ngoc Bich, Stem Cell Institute, University of Science Ho Chi Minh City, Viet Nam

Email: ngocvu@sci.edu.vn; vbngoc@hcmus.edu.vn

History

- Received: Jan 14, 2026
- Accepted: May 09, 2026
- Published Online: May 31, 2026

DOI : 10.15419/58ss7g56

Check for updates

INTRODUCTION

Psoriasis is a prevalent chronic skin inflammatory autoimmune disease without definitive cure. It affects both sexes and can occur at any age, with peak incidence observed between 50 to 69 years[1]. The disease typically exhibits a bimodal onset, occurring first between 20 to 39 years and again in life between 50 to 69 years. Its global prevalence ranges from 0.91% to 8.5%, depending on geographic and genetic factors[2]. Beyond cutaneous manifestations, psoriasis is associated with significant psychological burden and systemic complications, with approximately 23.8% of patients developing psoriatic arthritis[3].

Clinically, psoriasis is characterized by sharply demarcated erythematous plaques covered with silvery scales, which may be localized or widespread and are often accompanied by pruritus or burning sensations[4]. Histopathologically, the disease exhibits hallmark features including hyperkeratosis, parakeratosis, epidermal acanthosis, dilated tortuous vessels, and dense inflammatory infiltrate predominantly composed of lymphocytes[5]. Although current topical and systemic therapies, including biologics, have improved disease management, they are often associated with high costs, adverse effects, and disease relapse, highlighting the need for safe and more durable therapeutic strategies.

The pathogenesis of psoriasis is now understood as a complex, self-amplifying inflammatory network involving dynamic interactions between keratinocytes and immune cells. Environmental triggers can induce keratinocyte stress, leading to the release of antimicrobial peptides such as LL37, which activate dendritic cells (DCs). Activated DCs subsequently promote the differentiation of naïve T cells into Th1 and Th17 subsets. Th1 cells secrete interferon-gamma (IFN-γ) and tumor necrosis factor-alpha (TNF-α), while Th17 cells produce interleukin-17 (IL-17), collectively driving keratinocyte hyperproliferation and sustaining chronic inflammation[6,7].

Cite this article : Thu Thi-Hong D, Phuc Van P, Ngoc Bich V. **Localized subcutaneous injection of human umbilical cord derived mesenchymal stem cells attenuates psoriasis-like inflammation in an imiquimod-induced mouse model**. *Biomed. Res. Ther.* 2026, 13(05):8558-8572.

Among the various inflammatory pathways implicated, the IL-23/IL17 axis plays a central role in psoriasis pathogenesis and emerged as a critical therapeutic target[8,9]. IL-23, primarily secreted by activated DCs, promotes the differentiation, expansion, and maintenance of Th17 cells, thereby sustaining IL-17 production. In turn, IL-17 acts directly on keratinocytes to induce the production of proinflammatory cytokines, chemokines, and antimicrobial peptides, establishing a feed-forward inflammatory loop[10–12]. The clinical success of biologics targeting IL-17 and IL-23 further underscores the importance of this axis in disease progression[13–15].

The imiquimod (IMQ)-induced psoriasis mouse model, first established in 2009, is a well-recognized and widely used experimental system for studying psoriasis. Topical application of IMQ induces skin inflammation that closely resembles human psoriasis in terms of strongly dependent on the IL-23/IL-17 axis, making it particularly suitable for evaluating immunomodulatory therapies targeting this pathway[16].

Mesenchymal stem cells (MSCs) are multipotent stromal cells with well-documanted immunomodulatory properties. MSCs secrete a wide range of bioactive factors, including prostaglandin E2 (PGE2), indoleamine 2,3-dioxygenase (IDO), interleukin-10 (IL-10), and transforming growth factor – beta (TGF-β), which collectively suppress the activation and differentiation of Th17 and Th1 cells and inhibit DCs maturation[17–21]. Additionally, MSCs can induce macrophages polarization toward and anti-inflammatory phenotype, futher contributing to immune regulation[22,23]. These properties have led to increasing interest in MSC-based therapies for immune-mediated disease, including graft versus host disease, inflammatory bowel, and psoriasis[24].

Previous studies have demonstrated that MSC derived from various tissue sources, such as gingiva and dental pulp, can alleviate psoriasis-like inflammation in IMQ-induced model, primarily through suppression of Th1/Th17-associated cytokines and modulation of immune cell infiltration. However, therapeutic outcomes appear to vary depending on the cell source, culture conditions, and administration route[25,26]. In particular, the effects of localized versus systemic delivery remain incompletely understood.

Human umbilical cord-derived MSCs (hUC-MSCs) represent a promising cell source due to their low immunogenicity-attributed to minimal expression of costimulatory molecules such as CD80, CD86, and HLA-DR -as well as their high proliferative capacity and ethical accessibility[27]. Despite these advantages, the immunomodulatory effects of locally administered hUC-MSCs on key inflammaroty pathways in psoriasis, especially the IL-23/IL-17 axis, have not been fully elucidated.

Therefore, this study aims to investigate whether localized subcutaneous administration of hUC-MSCs can attenuate psoriasis-like inflammation in an IMQ-induced mouse model. Specifically, we focus on evaluating the modulation of proinflammatory cytokines associated with the IL-23/IL-17 axis, thereby providing additional evidence supporting the therapeutic potential of hUC-MSCs in psoriasis.

MATERIALS AND METHODS

Culture and characterization of hUC-MSCs

The hUC-MSCs were cultured and expanded in MSCCult I medium (Regenmedlab, Ho Chi Minh City, Vietnam) at 37 ℃ in a humidified atmosphere containing 5% CO_2. Cells at passage 7 (P7) were used for all experiments.

Prior to in vivo administration, hUC-MSCs were characterized in accordance with the minimal criteria established by the International Society for Cell & Gene Therapy (ISCT).

For injection, cells were prepared as a single-cell suspension. Briefly, adherent cells were detached using Deattachment solution (Regenmedlab, Ho Chi Minh City, Vietnam), followed by centrifugation at 500 × g for 5 min. The cell pellet was resuspended in phosphate-buffered saline (PBS). Cell viability was assessed using the trypan blue exclusion assay and was consistently greater than 90% at the time of injection. Cells were adjusted to a final concentration of 2.5 × 10^6 cells in 200 µL PBS per dose.

Differentiation assays

hUC-MSCs were detached by incubation at 37°C for 2 minutes using Deattachment solution (Regenmedlab, Ho Chi Minh City, Vietnam). The cells were then centrifuged at 500 x g for 5 min, and the resulting pellets were resuspended in MSCCult I medium. Subsequently, the cells were seeded into 96-well plate at a density of 1x10^4 cells per well in 200 µL of medium. After 24 hours, the culture medium was replaced with lineage-specific differentiation media. For osteogenic differentiation, hUC-MSCs were cultured in StemPro™ Osteogenesis Differentiation Kit (Thermo Scientific, Waltham, MA, USA) for 21

days. Chondrogenic differentiation was induced using StemPro™ Chondrogenesis Differentiation Kit (Thermo Scientific, Waltham, MA, USA) for 28 days. Adipose differentiation was performed by culturing hUC-MSCs in Adipogenesis Diffmed (Regenmedlab, Ho Chi Minh city, Vietnam) for 14 days. The differentiation media were refreshed every seven days.

At the end of the differentiation periods, cells were fixed in 4% paraformaldehyde (Sigma Aldrich, USA) and stained with Alizarin Red S (Sigma-Aldrich, St. Louis, MO, USA) to detect calcium accumulation, Alcian Blue (Sigma-Aldrich, St. Louis, MO, USA) to assess proteoglycan accumulation, and Oil Red O dye (Sigma-Aldrich, St. Louis, MO, USA) to detect the presence of lipid droplets.

Immunophenotyping of hUC-MSCs

For immunophenotypic analysis, human umbilical cord–derived mesenchymal stem cells (hUC-MSCs) at passage 7 (P7) were harvested and resuspended in phosphate-buffered saline (PBS). Cells were incubated with fluorochrome-conjugated monoclonal antibodies against CD44 (clone DB105, #130-113-342), CD73 (clone AD2, #130-120-066), CD90 (clone REA897, #130-114-860), CD105 (clone REA794, #130-112-170), CD14 (clone TÜK4, #130-113-146), CD34 (clone AC136, #130-113-178), and HLA-DR (clone AC122, #130-113-401) (all from Miltenyi Biotec, Germany) at a dilution of 1:100 for 15–20 minutes at room temperature in the dark.

Following incubation, cells were washed with PBS to remove unbound antibodies and analyzed using a flow cytometer (BD FACSCalibur™, BD Biosciences, USA) with BD CellQuest™ Pro software.

During analysis, cell populations were initially gated based on forward scatter (FSC) and side scatter (SSC) to exclude debris. The main cell population was then selected for further analysis. At least 10,000 events were acquired per sample. Unstained controls were used to define background fluorescence.

Cell viability assessment

Cell viability was determined immediately prior to administration using trypan blue exclusion assay. Only cell suspensions with viability greater than 90% were used for in vivo injection to ensure consistency and reliability of therapeutic outcomes.

Psoriasis Mouse Model and Cell Treatment

BALB/c male mice (8–12 weeks old) were housed under standard conditions with a 12 hour light/dark cycle and ad libitum access to food and water. All animal procedures were approved by the Animal Ethics Committee of Stem Cells Institute, University of Science, VNU-HCM (No. 230107/SCI-AEC) and conducted in accordance with relevant institutional guidelines.

Mice were randomly assigned to five groups (n=6 per group): (i) normal group (Normal); (ii) IMQ-induced group (IMQ); (iii) PBS-treated IMQ group (PBS);[28] hUC-MSC-treated IMQ group (hUC-MSCs); and (v) corticosteroid-treated IMQ group[29].

One day prior to treatement (day -1), dorsal hair was shaved. Day 0 was defined as the first day of IMQ application, representing the initiation of psoriasis-like inflammation.

For psoriasis induction, mice in the IMQ groups received a daily topical application of 5% Imiquad cream (Glenmark Pharmaceuticals Limited, Maharashtra, India; 63 mg of 5% cream per mouse, equivalent to 3.15 mg IMQ) on the dorsal skin for consecutive 6 days (day 0 to day 5). The cream was evenly applied using a sterile spatula and allowed to absorb for approximately 10–15 min before the animals were returned to their cages.

On day 2 (D2), mice in the PBS group received a subcutaneous injection of 200 µL PBS, while mice in the hUC-MSCs treatment group received a subcutaneous injection of hUC-MSCs (2.5×10^6 cells suspended in 200 µL PBS). The injection was administered locally into the dorsal skin at the site of IMQ application. Mice in the Cort group were treated with topical corticosteroid (Dermavate 0.05%, Glaxo Operations UK Limited, London, UK; 20 mg) from day 2 to day 5.

Euthanasia and tissue collection

Mice were euthanized on days 6 and 12. Euthanasia was performed by carbon dioxide (CO_2) inhalation using a gradual fill method. Briefly, animals were placed in a euthanasia chamber and exposed to CO_2 with a controlled displacement rate (approximately 20–30% of chamber volume per minute) until loss of consciousness, followed by continued exposure for at least 1–2 minutes after respiratory arrest to ensure death. Death was confirmed by cessation of respiration and lack of response to physical stimuli prior to tissue harvesting. Dorsal skin samples were then collected for subsequent analyses.

Experimental design and sample allocation

A total of 6 mice per group were included in this study and followed longitudinally. Non-terminal

parameters, including clinical scoring and skin thickness measurements, were assessed in all animals (n = 6 per group) from day 0 to day 6.

At day 6, a subset of mice (n = 3 per group) was randomly selected and euthanized for tissue collection, including histological, gene expression, and immunofluorescence analyses. The remaining mice (n = 3 per group) were further monitored from day 7 to day 12 and subsequently euthanized on day 12 for endpoint analyses.

Thus, terminal assays at each time point (day 6 and day 12) were performed using independent biological samples (n = 3), whereas longitudinal measurements prior to day 6 were conducted with n = 6 per group. No animals were reused across terminal endpoints.

Psoriasis Area and Severity Index (PASI) scoring

Disease severity was evaluated daily using a modified PASI scoring system assessing erythema, scaling, and skin thickness. Erythema and scaling were each scored on a scale from 0 to 4 as follows: 0, none; 1, slight; 2, moderate; 3, marked, and 4, very marked. Skin thickness was scored on the percentage increase relative to baseline (day 0) as follows: 0, no increase; 1, 15 - 20%; 2, 20 – 40%; 3, 40 – 60%; 4, >60%. The cumulative PASI score was calculated as the sum of erythema, scaling, and thickness score, with a maximum score of 12.

Immunohistochemistry

Skin samples were fixed in 4% paraformaldehyde (Sigma-Aldrich, St. Louis, MO, USA), embedded in paraffin, and sectioned at a thickness 4 µm. Tissue sections were deparaffinized in xylene (5 minutes, twice) and rehydrated through a graded ethanol series (100%, 95%, and 80%) before rinsing in distilled water

The sample sections were incubated in 10% goat serum for 30 minutes at room temperature to block nonspecific binding sites. After removing excess serum, the sections were incubated with diluted primary antibodies, including IL-17 (1:200, Cat#PA5-106856, Thermo Scientific, Waltham, MA, USA) and IL-23p19 (1:200, Cat#PA5-20239, Thermo Scientific, Waltham, MA, USA) for 30 minutes at room temperature. Subsequently, the slides were gently washed with phosphate-buffered saline (PBS) and treated with Goat Anti-Rabbit (IgG) secondary antibody FITC (1:200, Cat#ab6717, Abcam Limited, Cambridge, UK) for 30 minutes at room temperature, followed by another PBS wash. Finally, the sections were mounted with Invitrogen™ Fluoromount-G™ Mounting Medium, with DAPI (1:20, Cat#00-4959-52, Thermo Scientific, Waltham, MA, USA) and observed using an Observer A1 microscope (Zeiss, Germany). Image analysis was performed using ImageJ software.

Immunofluorescence image quantification

Immunofluorescence images were acquired under identical exposure settings using a fluorescence microscope (Observer A1, Zeiss, Germany) to ensure comparability across experimental groups. For each sample, 3–5 non-overlapping fields were randomly selected from comparable regions of the tissue section.

Quantitative analysis was performed using ImageJ software (NIH, USA). Images were converted to grayscale, and a consistent threshold was applied across all groups to define positive staining. Mean fluorescence intensity (MFI) and/or the percentage of positively stained area were quantified within regions of interest (ROIs) of equal size. Background fluorescence was subtracted using adjacent unstained regions.

RT-qPCR assay

Total RNA was isolated from mouse skin samples using the easy-BLUE™ Total RNA Extraction Kit (iNtRON Biotechnology, MA, USA) according to the manufacturer's instructions. RNA quantity and purity were assessed spectrophotometrically.

Gene expression analysis was quantified via reverse transcription-quantitative polymerase chain reaction (RT-qPCR) using the Luna® Universal SYBR Green One-Step RT-qPCR Kit (New England Biolabs, USA). Thermocycling conditions were followed as per the manufacturer's protocol. Cycle threshold (Ct) values were calculated and normalized to the housekeeping gene *GAPDH*. The primers used for gene expression analysis are listed in Table 1. Primer specificity was confirmed by melt curve analysis.

Cycle threshold (Ct) values were obtained and normalized to the housekeeping gene GAPDH to generate ΔCt values. Relative gene expression levels were calculated using the $2^{-\Delta\Delta Ct}$ method, with the normal (untreated) group serving as the calibrator.

For statistical analysis, ΔCt values were used to ensure appropriate handling of approximately normally distributed data, whereas relative expression values ($2^{-\Delta\Delta Ct}$) are presented for visualization.

Table 1: A list of primer sequences was used in this study.

Gene	Forward primer (5'-3')	Reverse primer (5'-3')	Length product (bp)
Il17a	AGCGTGTCCAAACACTGAGG	ACGTGGAACGGTTGAGGTAG	125
IL-23	TGGAGCAACTTCACACCTCC	GGCAGCTATGGCCAAAAAGG	170
Ifng	CCATCGGCTGACCTAGAGAA-GAC	GCCACTTGAGTTAAAATAGTTATTCA-GAC	224
Tnf	AAGCCTGTAGCCCACGTCGTA	GGCACCACTAGTTGGTTGTCTTT	122
Ccl20	CGACTGTTGCCTCTCGTACA	GAGGAGGTTCACAGCCCTTT	178
GapDH	GCATCTTCTTGTGCAGTGCC	TACGGCCAAATCCGTTCACA	74

Blinding procedure

Outcome assessments were conducted by an investigator independent of the experimental procedures to minimize potential bias. However, formal blinding through coded sample allocation was not implemented, which is acknowledged as a limitation of the study.

Statistical analysis

Data are presented as biological replicates (n = 3–6 mice per group, depending on the experimental endpoint). The entire experiment was independently repeated at least three times using separate cohorts of animals under identical conditions to ensure reproducibility.

Statistical analysis was conducted by GraphPad Prism software version 9.5.1. Data are presented as means ± standard error of the mean (SEM).

Statistical analysis was performed using two-way ANOVA followed by Tukey's multiple comparisons test. A p-value < 0.05 was considered statistically significant.

RESULTS

Culture and characterization of hUC-MSCs.

hUC-MSCs adhered to the flask surface, exhibiting an elongated spindle shape (Figure 1A). In the chondrogenic medium, hUC-MSCs formed clusters and displayed blue staining with Alcian Blue, demonstrating chondrogenic potential after 28 days (Figure 1B). After 21 days of culture in the osteogenic differentiation medium, Alizarin Red staining revealed calcium accumulation, indicating osteogenesis (Figure 1C). Additionally, adipogenic differentiation was confirmed by the presence of lipid droplets stained red with Oil Red O dye after 14 days (Figure 1D).

Flow cytometry analysis showed that hUC-MSCs were positive for CD44 (99.28%), CD73 (99.50%), CD90 (99.20%), and CD105 (99.91%), while negative for CD14 (0.11%), CD34 (0.16%), and HLA-DR (0.83%) (Figure 1E).

hUC-MSCs alleviated symptoms in the IMQ-induced psoriasis mice model

In the normal group (Figure 2A1–A6) and on day 0 in all treatment groups (Figure 2B1–E6), no signs of erythema, irritation, or inflammation were observed, suggesting that the procedures did not induce adverse skin reactions.

In contrast, mice in the IMQ group exhibited a progressive development of psoriasis-like symptoms. Erythema appeared as early as day 1, accompanied by increased skin thickness and mild inflammation. By day 3, scaling became evident, and a dark red rash covered the dorsal skin, along with silvery scales and peeling. Clinical severity peaked on day 6, with widespread thickening, scaling, and pronounced erythema (Figure 2B4, C4, D4, E4). On days 5 and 6, the back skin was covered with thick silver-white scales, and skin thickness markedly increased. The Psoriasis Area and Severity Index (PASI) reached its maximum score of 11–12 during this period (Figure 3D). The total PASI score in the IMQ group remained significantly elevated compared to the normal group from day 1 to day 12 ($p < 0.05$).

hUC-MSCs Treatment Alleviates Clinical Severity in the IMQ-Induced Psoriasis Model

In the IMQ and PBS groups, all clinical parameters progressively worsened following IMQ application. Skin thickness increased markedly from day 1 and peaked around day 5-6, followed by a decline after cessation of IMQ treatment (after day 6) (Figure 3A). Similarly, erythema and scaling score increase overtime, with maximal severity observed between days 5 and 6 (Figure 3B–C). The cumulative PASI score reached 11–12 points in both IMQ and PBS groups, indicating severe disease activity (Figure 3D). After

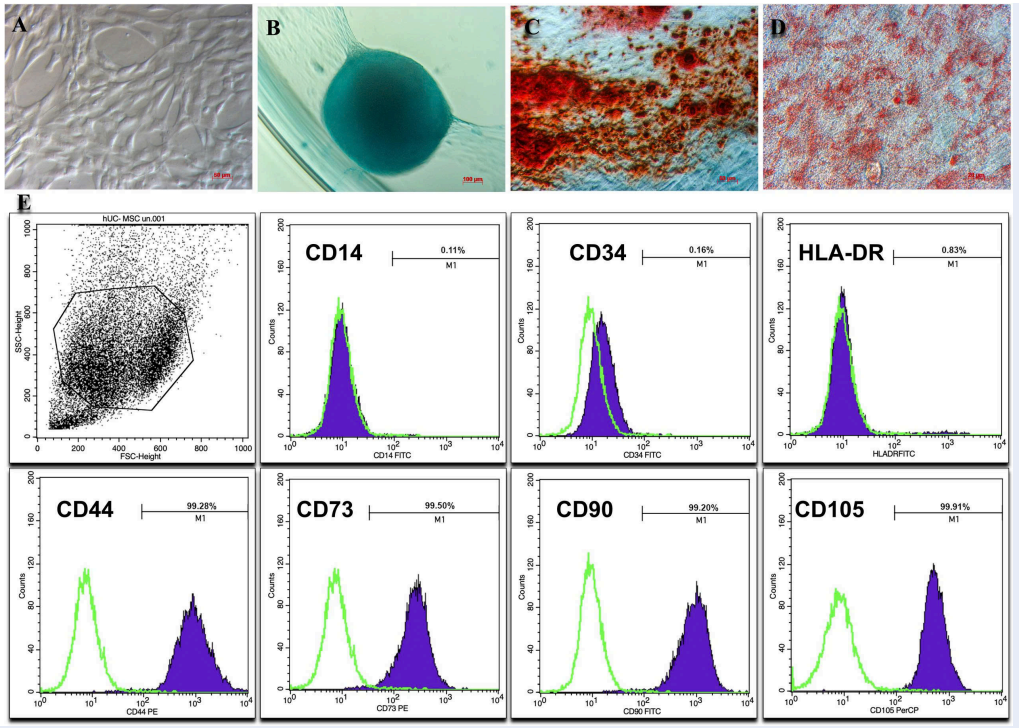

Figure 1: **The characteristics of hUC-MSCs**. (A) Morphology of hUC-MSCs under phase-contrast microscopy. (B–D) Multilineage differentiation of hUC-MSCs: chondrogenic differentiation on day 28 stained with Alcian Blue (B), osteogenic differentiation on day 21 stained with Alizarin Red (C), and adipogenic differentiation on day 14 stained with Oil Red O (D).(E) Flow cytometry analysis shows high expression of MSC surface markers CD44, CD73, CD90, and CD105 (>95%) and negative expression of CD14, CD34, and HLA-DR (<2%).Data are representative of three independent experiments (n = 3).

IMQ withdrawal, clinical symptoms gradually subsided; however, residual erythema and scaling were still evident in the PBS group at day 12, suggesting incomplete resolution.

In contrast, mice treated with hUC-MSCs exhibited attenuated disease progression. Reductions in skin thickness and erythema were observed from approximately day 5–6 onward, with a more rapid decline compared to PBS group ($p<0.05$) (Figure 3A-B). The scaling score was also significantly reduced beginning on day 5 ($p < 0.05$) (Figure 3C). The cumulative PASI score in the hUC-MSCs group remained consistently lower than in the IMQ and PBS groups, with a peak of 7–8, corresponding to an approximate 33% reduction compared to PBS controls ($p < 0.05$) (Figure 3D). By day 12, clinical scores in the hUC-MSCs group approached baseline levels.

Treatment with Cort produced comparable improvements. Clinical parameters in Cort group followed a similar trajectory to the observed in the hUC-MSCs group, with accelerated resolution during the recovery phase (day 7–12). No statistically significant differences were observed between the hUC-MSCs and Cort groups across all clinical parameters throughout the study period ($p > 0.05$).

Collectively, these results demonstrate that hUC-MSCs administration attenuates psoriasis-like skin inflammation in the IMQ-induced mouse model, as evidenced by reduced peak disease severity and accelerated resolution following IMQ withdrawal.

Histological Restoration of Psoriatic Skin by hUC-MSCs Treatment

Histological evaluation of dorsal skin tissues on days 6 and 12 revealed marked structural differences among experimental groups (Figure 4A–K).

In the normal control group, skin architecture remained intact at both time points (Figure 4A, G), characterized by a thin epidermis (19.57 ± 3.35 μm) composed of 2–3 layers of keratinocytes layer, a well-organized dermis with densely collagen fibers, and preserved skin appendages, including hair follicles and sebaceous glands (green arrows). No pathological alteration was observed.

In contrast, the IMQ group exhibited characteristic psoriasis features on day 6 (Figure 4B), includ-

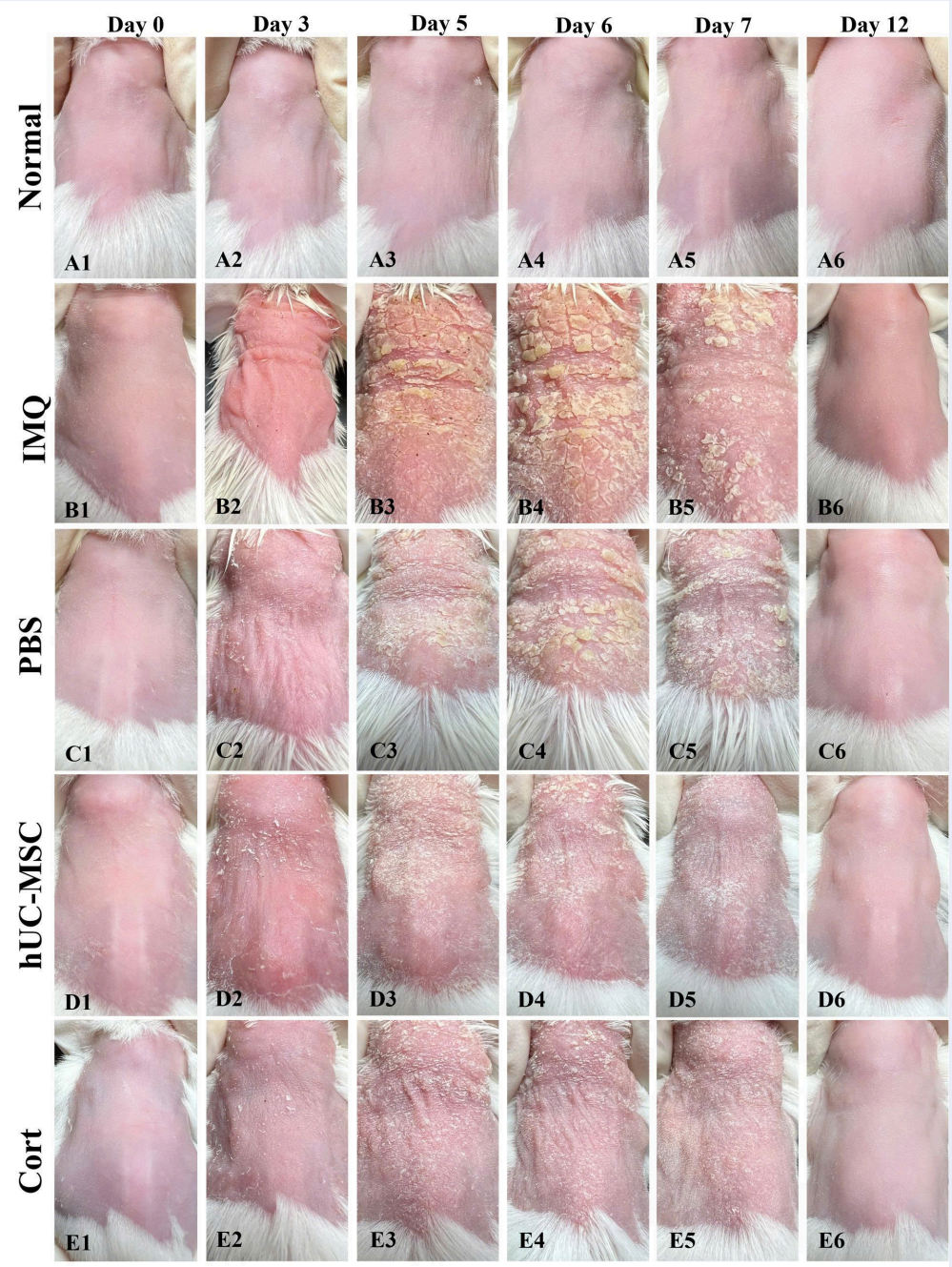

Figure 2: **Clinical presentation of psoriasis-like skin lesions in mice.** Sequential images of dorsal skin at defined time points (day 0, 2, 4, 6, and 12) normal mice (A1–A6), IMQ-induced mice (B1–B6), PBS-treated mice (C1–C6), hUC-MSCs-treated mice (D1–D6), and Cort-treated mice (E1–E6), illustrating erythema, scaling, and thickening progression or resolution. Day 0 represents the time point immediately after hair removal and the first application of IMQ. IMQ was applied daily from day 0 to day 5. Images are representative of biological replicates (n = 6 per group for days 0–6; n = 3 per group for day 7 and 12).

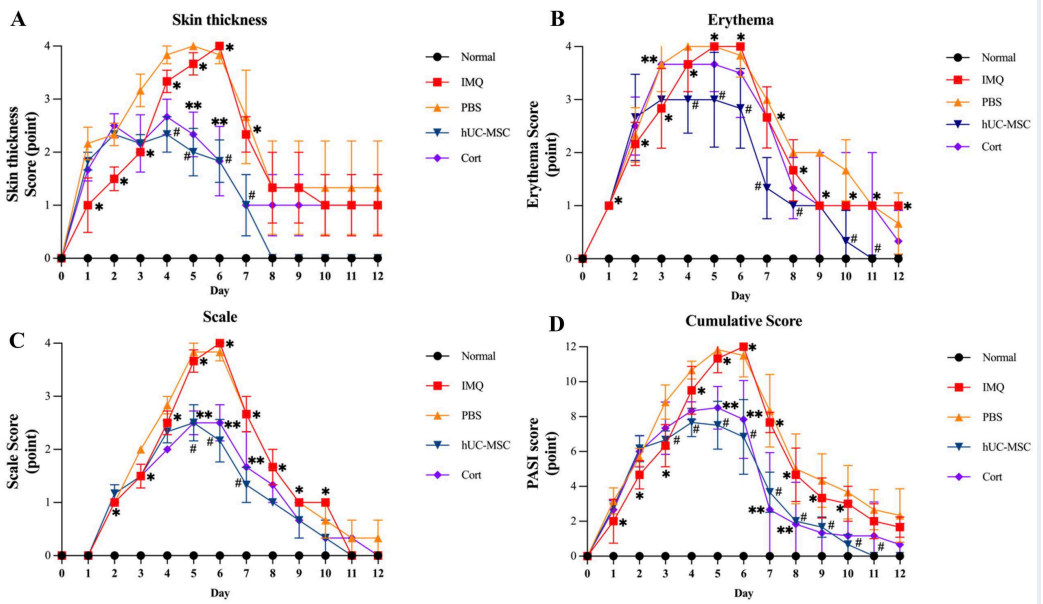

Figure 3: Clinical severity of IMQ-induced psoriasis-like dermatitis and therapeutic effects of hUC-MSCs. Longitudinal assessment of psoriasis-like symptoms, including (A) skin thickness, (B) erythema, (C) scaling, and (D) cumulative PASI score in Normal, IMQ, PBS, hUC-MSC, and corticosteroid[29] groups from day 0 to day 12. Day 0 was defined as the first day of IMQ application following hair removal. IMQ was applied daily from day 0 to day 5, and treatments were administered on day 2. Clinical severity increased progressively and peaked at days 5–6 in IMQ and PBS groups, followed by a resolution phase after IMQ withdrawal. Treatment with hUC-MSCs or Cort attenuated disease severity and accelerated recovery compared to PBS controls. Non-terminal assessments (clinical scoring and skin thickness) were performed in all animals from day 0 to day 6 (n = 6 per group). At day 6, a subset of mice (n = 3 per group) was euthanized for tissue collection, while the remaining mice (n = 3 per group) were monitored until day 12. Thus, longitudinal data from day 0–6 represent n = 6, whereas data from day 7–12 represent n = 3 independent biological samples. Data are presented as mean ± SEM. Statistical analysis was performed using two-way repeated-measures ANOVA followed by multiple comparisons tests. *p<0.05, normal vs IMQ group; #p<0.05, PBS vs hUC-MSC group; **p<0.05, IMQ vs Cort group).

ing pronounced epidermal hyperplasia (116.48 ± 6.57 μm), elongation of rete ridges, loss of the granular layer, and marked inflammatory cell infiltration (Figure 4C). Adition hallmarks, parakeratosis, Munro microabscesses, and vascular dilation were also observed (Figure 4C). Although partial resolution was evident by 12 (Figure 4H), epidermal thickness and dermal inflammation remained elevated compared to the normal group.

The PBS group displayed histologically feature comparable to those of the IMQ group, with severe epidermal thickness on day 6 (120.05 ± 12.45 μm) and only partial improvement by day 12 (Figure 4D, I), indicating the absence of a therapeutic effect.

In the hUC-MSCs group, a marked attenuation of psoriasis feature was observed. On day 6, epidermal thickness was significantly reduced to 39.40 ± 3.31 μm compared to the PBS group ($p < 0.001$ vs.), accompanied by decreased parakeratosis, reduced inflammation infiltration, and diminished vascular dilation (Figure 4E). By day 12 (Figure 4J), the skin architecture was largely restored, with minimal residual abnormalities and morphology approaching that of the normal group.

Similarly, the Cort group also demonstrated substantial histological improvement, with reduced epidermal thickness (49.58 ± 4.89 μm) on day 6 and near-complete restoration of skin structure by day 12 (Figure 4F, K). The extent of recovery was comparable to that observed in the hUC-MSCs group

Quantitative analysis of epidermal thickness (Figure 4L) confirmed significant differences among groups. Both hUC-MSCs and Cort groups resulted in significantly lower epidermal thickness compared to PBS and IMQ groups ($p < 0.01$), with no significant difference observed between hUC-MSC and Cord Group.

Collectively, these findings indicate that hUC-MSCs treatment effectively attenuate IMQ-induced histopathological alterations, as reflected by reduced epidermal hyperplasia and inflammation features.

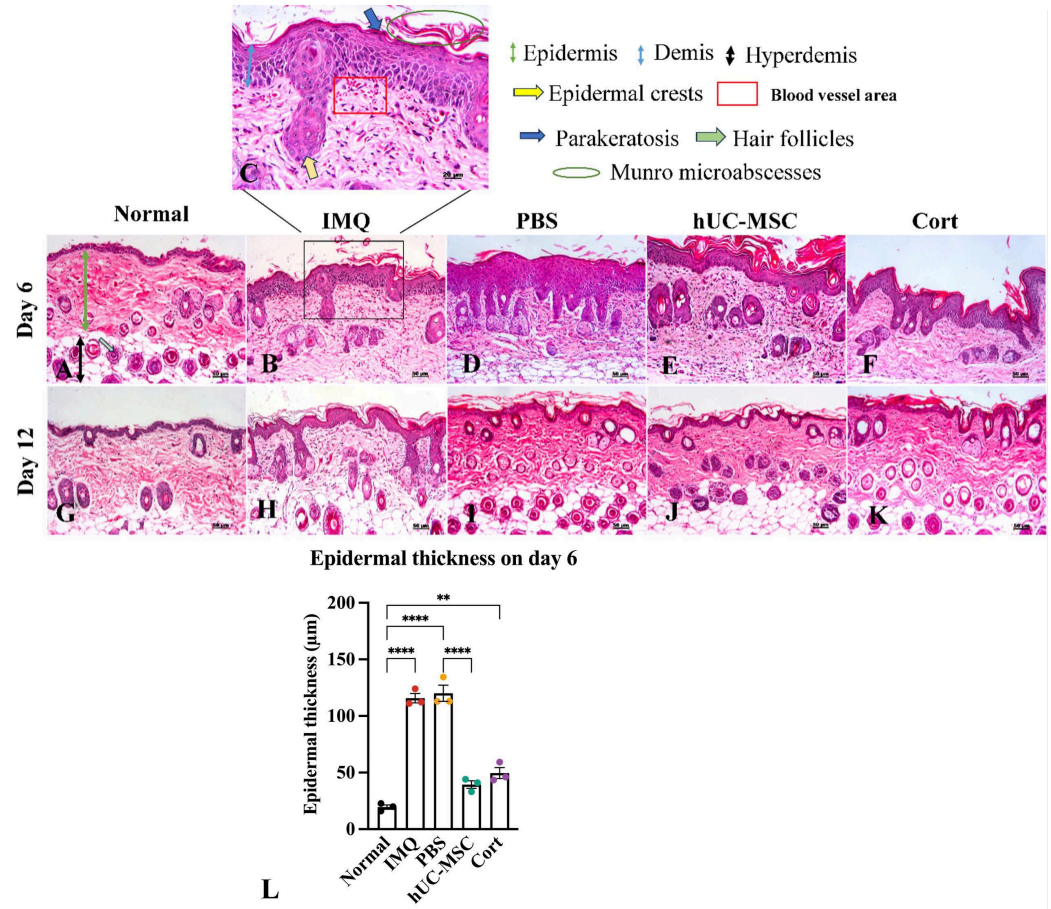

Figure 4: Histological evaluation of skin lesions in the IMQ-induced psoriasis model. Hematoxylin and eosin (H&E) staining of dorsal skin sections from Normal (A, G), IMQ (B, H), PBS (D, I), hUC-MSC (E, J), and corticosteroid-treated (Cort; F, K) groups at day 6 (A–F) and day 12 (G–K). Representative psoriatic features, including parakeratosis and Munro microabscesses, are shown in panel (C). Scale bar: 50 μm. (L) Quantification of epidermal thickness across groups. Data are presented as mean ± SEM (n = 3 per group per time point). Statistical analysis was performed using one-way ANOVA followed by multiple comparisons tests. *** $p < 0.001$; **** $p < 0.0001$.

hUC-MSCs Suppress IL-17A and IL-23 Expression in Psoriatic Skin

To evaluate the anti-inflammatory effects of hUC-MSCs, IL-17A and IL-23 expression in skin lesions was assessed by immunofluorescence staining and semi-quantitative image analysis on 6 and day 12 (Figure 5A–C).

IL-17A and IL-23 signals (green) were predominantly localized in the epidermis and upper dermis, while nuclei were counterstained with DAPI (blue). In the normal group, both cytokines were absent or minimally detected at both time points, indicating basal expression levels.

In contrast, the IMQ group exhibited strong IL-17A and IL-23 signals on day 6, particularly within the epidermis and dermal inflammatory infiltrates, consistent with active psoriatic inflammation. Similar expression patterns were observed in the PBS group, indicating a lack of therapeutic effect. By day 12, cytokine expression decreased compared to day 6 but remained elevated relative to the normal group, suggesting incomplete resolution.

In the hUC-MSC-treated group, a marked reduction in IL-17A and IL-23 expression was observed on day 6, with fewer positive cells detected in both epidermal and dermal regions. By day 12, cytokine signals were further reduced and approached those observed in the normal group. A similar trend was observed in the Cort group, with reduced cytokine expression at day 6 and further attenuation by day 12. Semi-quantitative analysis of fluorescence intensity (Figure 5B, C) supported these observations. On day 6, IL-17A and IL-23 levels were significantly increased in the IMQ and PBS groups compared to the

normal group, whereas hUC-MSC treatment significantly reduced cytokine expression ($p < 0.05$). By day 12, fluorescence intensities declined across all groups, and no significant differences were observed between the hUC-MSC, Cort, and normal groups ($p > 0.05$).

Together, these results indicate that hUC-MSC treatment is associated with reduced expression of IL-17A and IL-23 in psoriatic skin, consistent with attenuation of inflammatory responses.

hUC-MSCs Attenuate the Expression of Psoriasis-Associated Inflammatory Genes

On day 6, IMQ-treated mice exhibited significant upregulation of proinflammatory genes compared to the normal group ($p < 0.05$), confirming successful induction of psoriasis-like inflammation. The relative expression levels were markedly increased for *Il17a* (130.39 ± 21.67), *Il23* (8.16 ± 2.75), *Ifng* (4.26 ± 0.82), *Tnf* (6.15 ± 1.15), and *Ccl20* (3.68 ± 1.17) (Figure 6).

In the PBS-treated group, expression levels remained elevated and were not significantly different from those in the IMQ group ($p > 0.05$), indicating a lack of therapeutic effect. Notably, *Tnf* expression was further increased in the PBS group (17.30 ± 2.78, $p < 0.01$ vs IMQ), accompanied by a trend toward increased *Ccl20* expression, which may reflect local responses to injection or tissue manipulation.

In contrast, hUC-MSC treatment resulted in a marked reduction in inflammatory gene expression. The most pronounced effects were observed for *Tnf* (0.9 ± 0.3, $p < 0.0001$ vs PBS) and *Ccl20* (1.0 ± 0.2, $p < 0.05$ vs PBS). Reductions in *Il17a* (39.28 ± 17.56), *Il23* (3.53 ± 0.23), and *Ifng* (2.16 ± 0.20) were also observed; however, these changes were less pronounced and did not consistently reach statistical significance, suggesting a moderate effect on upstream cytokine expression within the IL-23/IL-17 axis.

A similar suppression pattern was observed in the Cort-treated group, with no statistically significant differences between hUC-MSC and Cort treatments ($p > 0.05$).

By day 12, expression levels of all genes decreased across groups and approached baseline, with no significant differences detected between treated and untreated groups ($p > 0.05$), consistent with the self-limiting nature of IMQ-induced inflammation.

Overall, these results indicate that hUC-MSC treatment is associated with reduced expression of key inflammatory mediators in psoriatic skin, particularly *Tnf* and *Ccl20*.

DISCUSSION

Psoriasis is a complex immune-mediated skin disorder characterized by dysregulated interactions between keratinocytes and immune cells. In the present study, subcutaneous administration of hUC-MSCs significantly attenuated psoriasis-like manifestations in an IMQ-induced mouse model, as evidenced by improvements at clinical, histological, and molecular levels[4,5].

Consistent with previous reports, IMQ application induced a robust psoriasis-like phenotype, with peak disease severity observed around day 5–6. This was reflected by increased PASI scores, marked epidermal hyperplasia, and elevated expression of key inflammatory mediators, including *Il17a*, *Il23*, *Ifng*, *Tnf*, and *Ccl20*. These changes align with the known activation of the IL-23/IL-17 axis in IMQ-driven inflammation and support the validity of the model for evaluating anti-inflammatory interventions[30–32].

In this study, hUC-MSCs at passage 7 (P7) were used. Although extended in vitro expansion has been associated with cellular senescence and potential phenotypic alterations, previous studies have reported that MSCs within the range of early to mid-passages (typically up to P8) generally retain their characteristic morphology, immunophenotype, and functional properties[33,34]. Consistent with this, the hUC-MSCs used in the present study fulfilled the minimal criteria defined by the International Society for Cell & Gene Therapy, including surface marker expression and trilineage differentiation capacity[29]. Nevertheless, we acknowledge that higher passage numbers may introduce subtle biological changes that were not specifically assessed in this study. Future investigations incorporating senescence-related markers and comparative analyses across passages would provide further insight into the impact of in vitro expansion on therapeutic efficacy.

Following hUC-MSC administration, a consistent therapeutic effect was observed across multiple levels of analysis. Clinically, hUC-MSC-treated mice exhibited reduced disease severity and faster resolution compared to PBS controls. Histologically, treatment was associated with decreased epidermal thickness and reduced inflammatory features. At the molecular level, both gene expression and protein analyses demonstrated reduced levels of IL-17A and IL-23, accompanied by downregulation of additional inflammatory mediators such as *Tnf* and *Ccl20*. The convergence of these findings across independent readouts strengthens the overall interpretation that hUC-MSCs exert a measurable anti-inflammatory effect in this model.

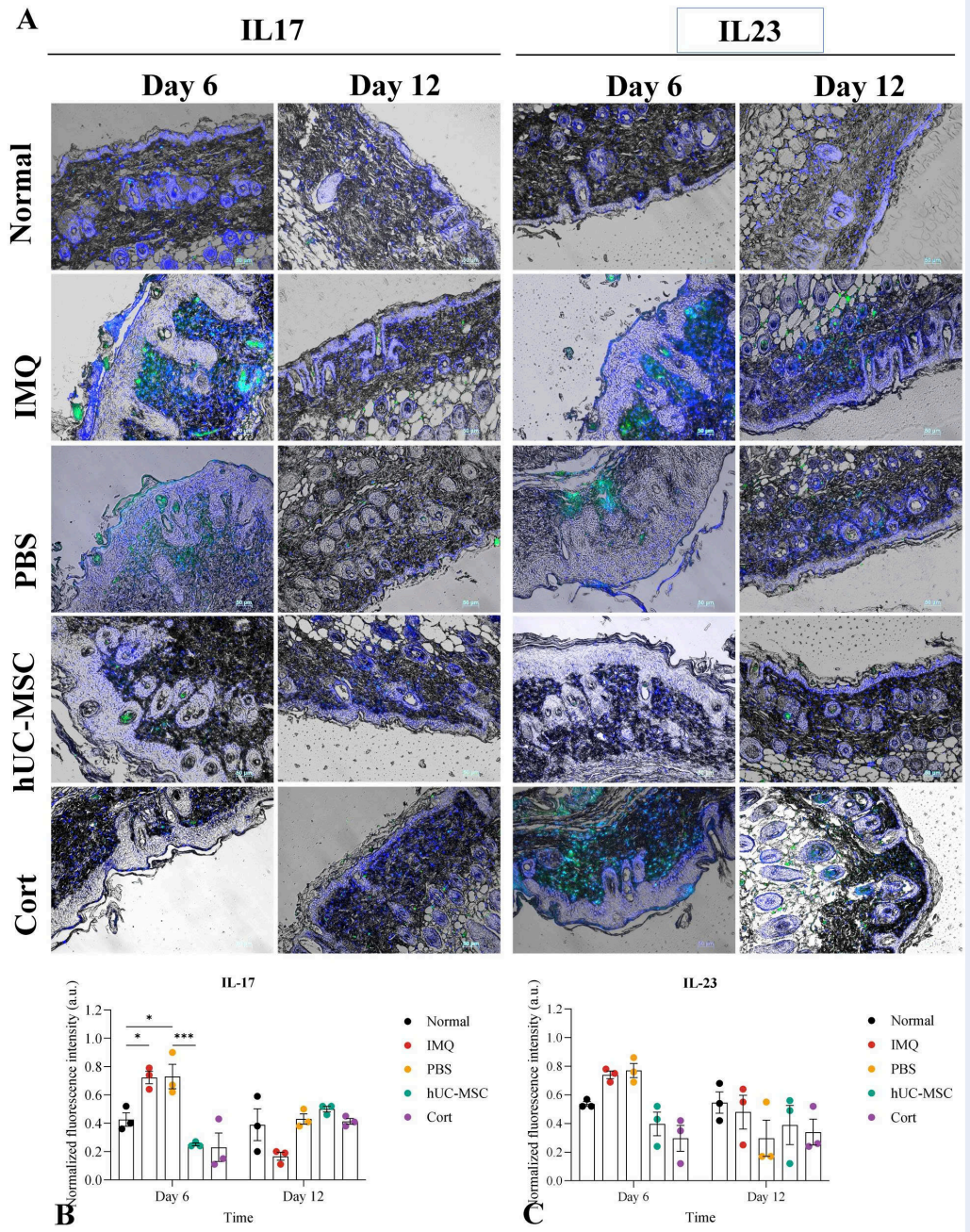

Figure 5: Effects of hUC-MSCs on IL-17A and IL-23 expression in psoriatic skin. (A) Representative immunofluorescence images of IL-17A and IL-23 expression in dorsal skin sections from Normal, IMQ, PBS, hUC-MSC, and corticosteroid-treated [29] groups at day 6 and day 12. Cytokines are shown in green, and nuclei are counterstained with DAPI (blue). Scale bars: 50 μm. (B, C) Semi-quantitative analysis of fluorescence intensity for IL-17A (B) and IL-23 (C). Data are presented as mean ± SEM (n = 3 biological replicates per group per time point). Statistical analysis was performed using two-way ANOVA followed by multiple comparisons tests. *p < 0.05; ***p < 0.001.

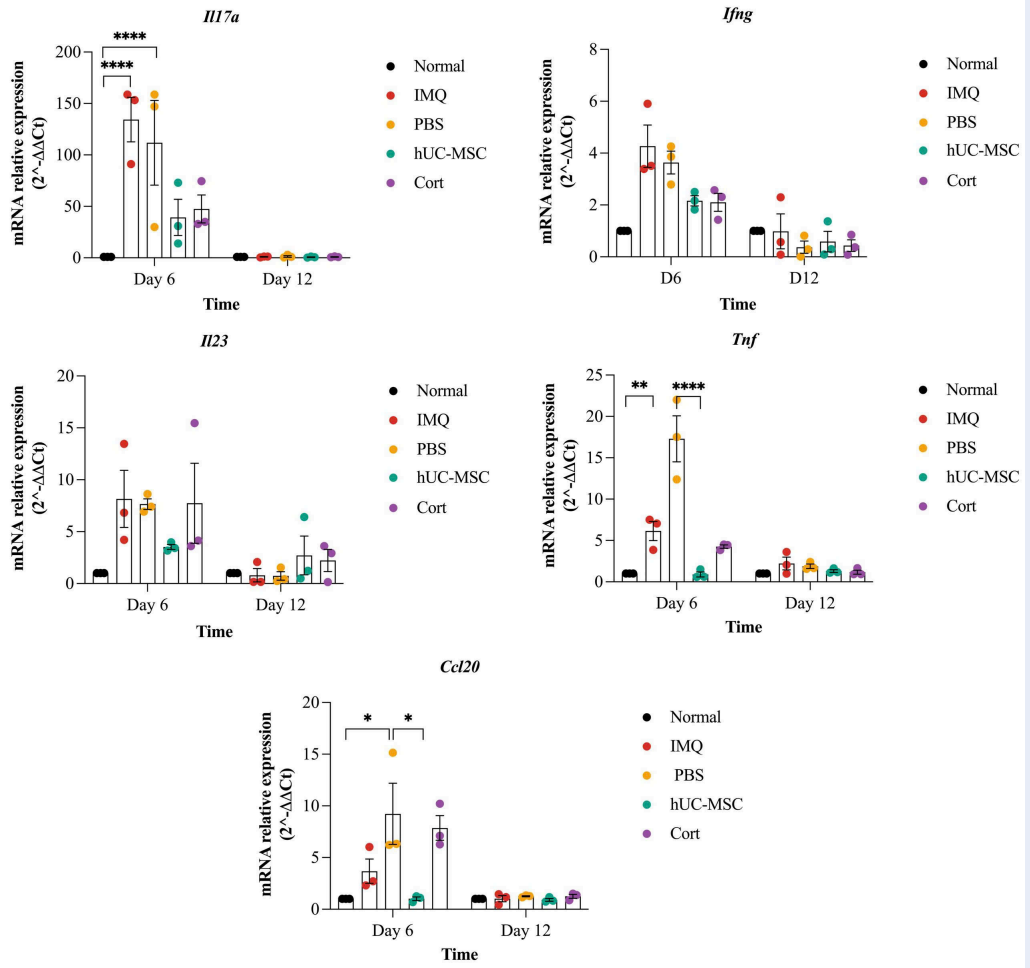

Figure 6: **hUC-MSCs attenuate psoriasis-related pro-inflammatory gene expression.** Relative mRNA expression of Il17a, Il23, Ifng, Tnf, and Ccl20 in dorsal skin at days 6 (left panels) and 12 (right panels) following treatment. Expression levels were normalized to the normal control (set to 1). IMQ induced robust upregulation of inflammatory genes, which was not attenuated by PBS administration. hUC-MSC treatment significantly reduced expression of key mediators, with the strongest effects observed for Tnf and Ccl20. The Cort group showed comparable suppression. By day 12, expression levels declined across all groups and approached baseline. Data are presented as mean ± SEM (n = 3 biological replicates). Statistical significance was determined by two-way ANOVA with multiple comparisons (*p < 0.05; **p < 0.01; ***p < 0.005; ****p < 0.0001).

Notably, the magnitude of suppression was more pronounced for *Tnf* and *Ccl20* compared to upstream cytokines such as *Il17a* and *Il23*. This pattern may suggest that hUC-MSCs preferentially influence downstream inflammatory amplification and leukocyte recruitment processes rather than directly suppressing upstream cytokine production. However, given the descriptive nature of the present study, this interpretation should be considered cautiously and requires further mechanistic validation.

The observed therapeutic effects are consistent with the known immunomodulatory properties of MSCs, which include the secretion of anti-inflammatory mediators and the ability to modulate immune cell function[35–37]. Although the present study did not directly investigate the underlying mechanisms, potential pathways may involve paracrine signaling, including cytokines or extracellular vesicles, as well as indirect modulation of immune cell subsets such as T cells or macrophages[38]. Future studies incorporating lineage tracing, immune profiling, or secretome analysis will be necessary to delineate these mechanisms more precisely.

Importantly, the efficacy of hUC-MSCs observed in this study was comparable to that of corticosteroid treatment across multiple parameters. This

finding highlights the potential of hUC-MSCs as an alternative or complementary therapeutic strategy, particularly given their broader immunomodulatory profile. However, it should be emphasized that current biologic therapies targeting IL-17 and IL-23 have demonstrated high clinical efficacy and well-characterized mechanisms of action[39,40]. Therefore, while MSC-based approaches may offer multi-target effects, their relative advantages and translational potential require further validation in more clinically relevant settings.

The timing and route of administration may also contribute to the observed therapeutic effects. In this study, hUC-MSCs were delivered subcutaneously at an early stage of inflammation (day 2), which may have enabled modulation of the evolving immune response. Localized delivery may enhance site-specific effects while limiting systemic exposure; however, comparative studies with systemic administration routes are needed to determine optimal delivery strategies.

Despite these promising findings, several limitations should be considered. The IMQ-induced model primarily reflects an acute inflammatory response and does not fully recapitulate the chronic, relapsing nature of human psoriasis. As observed in this study, inflammatory and clinical parameters declined across all groups by day 12, indicating a self-limiting process. This limits the ability to assess long-term therapeutic durability.

Although PBS injection was included as a procedural control, the absence of a sham injection group prevents complete exclusion of mechanical or injection-related effects. The increased expression of certain inflammatory mediators, particularly Tnf, in the PBS group suggests that local tissue perturbation may contribute to transient inflammatory responses. While this observation supports the robustness of the suppressive effect observed with hUC-MSC treatment, it also highlights the need for more refined control conditions in future studies.

Additional limitations include the relatively small sample size for terminal analyses and the absence of mechanistic assays to identify the specific cellular targets of hUC-MSCs. The use of a single dose and a single administration time point further precludes conclusions regarding dose dependency or optimal treatment scheduling. Moreover, the lack of additional control groups, such as a naïve MSC-treated group, limits the ability to distinguish baseline immunomodulatory effects from treatment-specific responses.

Finally, longitudinal clinical data were analyzed using a two-way ANOVA framework in which measurements at each time point were treated as independent observations. While this approach enables comparison across groups and time, it may not fully account for within-subject correlations and should be considered a limitation of the current analysis.

Collectively, the present study demonstrates that localized administration of hUC-MSCs attenuates psoriasis-like inflammation in an IMQ-induced mouse model. The observed effects are supported by consistent improvements in clinical scoring, histopathological features, and inflammatory cytokine expression. These findings suggest that hUC-MSCs may represent a potential immunomodulatory approach for psoriasis, primarily through the attenuation of inflammatory responses rather than direct disease modification.

CONCLUSION

In this study, subcutaneous administration of hUC-MSCs significantly alleviated clinical and histopathological features of psoriasis-like dermatitis in an IMQ-induced mouse model. Treatment was associated with reduced epidermal hyperplasia, diminished inflammatory infiltration, and decreased expression of key cytokines, including IL-17A, IL-23, IFN-γ, TNF-α, and CCL20. These findings support the immunomodulatory effects of hUC-MSCs in acute inflammatory settings. However, given the limitations of the model and the absence of long-term evaluation, further studies are required to determine the durability, mechanism, and translational relevance of this approach in chronic psoriasis

ABBREVIATIONS

hUC-MSCs: Human umbilical cord mesenchymal stem cells; **IMQ**: Imiquimod; ***IFN-γ*** : Interferon-gamma; ***TNF-α*** : Tumour Necrosis Factor alpha; ***IL-17***: Interleukin 17; ***IL-23***: Interleukin 23; ***CCL20***: CC chemokine ligand 20; **Th17**: T helper 17 cell; **Th1**: T Helper 1 Cells; **PGE2**: Prostaglandin E2, **IDO** : Indoleamine 2,3-dioxygenase, **PASI**: Psoriasis Area and Severity Index, **IHC**: Immunohistochemistry, **GAPDH**: Glyceraldehyde 3 Phosphate Dehydrogenase

ACKNOWLEDGMENTS

This work was supported by Stem Cell Institute, University of Science, VNU-HCM.

AUTHOR'S CONTRIBUTIONS

Conceptualization: Ngoc Bich Vu (NBV), Phuc Van Pham (PVP). Data curation: Thu Thi-Hong Dao (TTHD), NBV. Formal analysis: TTHD, NBV. Investigation: TTHD, NBV. Methodology: TTHD, NBV. Project administration: NBV. Supervision: NBV. Validation: NBV, PVP. Visualization: NBV, PVP. Writing – original draft: TTHD, NBV. Writing – review and editing: NBV. All authors read and approved the final manuscript.

FUNDING

None.

AVAILABILITY OF DATA AND MATERIALS

Data and materials used and/or analyzed during the current study are available from the corresponding author on reasonable request.

ETHICS APPROVAL AND CONSENT TO PARTICIPATE

Not applicable.

CONSENT FOR PUBLICATION

Not applicable.

DECLARATION OF GENERATIVE AI AND AI-ASSISTED TECHNOLOGIES IN THE WRITING PROCESS

The authors declare that they have used generative AI and/or AI-assisted technologies in the writing process before submission, but only to improve the language and readability of their paper.

COMPETING INTERESTS

The authors declare that they have no competing interests.

REFERENCES

1. Damiani G, Bragazzi NL, Karimkhani Aksut C, et al. The Global, Regional, and National Burden of Psoriasis: Results and Insights From the Global Burden of Disease 2019 Study. Frontiers in Medicine (Lausanne). 2021;8:743180. Available from: https://doi.org/10.3389/fmed.2021.743180.
2. Parisi R, Symmons DP, Griffiths CE, Ashcroft DM. Global epidemiology of psoriasis: a systematic review of incidence and prevalence. Journal of Investigative Dermatology. 2013 Feb;133(2):377–385. Available from: https://doi.org/10.1038/jid.2012.339.
3. Alinaghi F, Calov M, Kristensen LE, et al. Prevalence of psoriatic arthritis in patients with psoriasis: A systematic review and meta-analysis of observational and clinical studies. Journal of the American Academy of Dermatology. 2019 Jan;80(1):251–265. Available from: https://doi.org/10.1016/j.jaad.2018.06.027.
4. Browning J. Dermatology Edited by Jean L. Bolognia, Julie V. Schaffer, Lorenzo Cerroni. Fourth edition. China: Elsevier, 2018, ISBN 978–0-7020–6275–9. Pediatric Dermatology. 2018;35(2):289–289. Available from: https://doi.org/10.1111/pde.13439.
5. Boehncke WH, Schön MP. Psoriasis. Lancet. 2015 Sep;386(9997):983–994. Available from: https://doi.org/10.1016/s0140-6736(14)61909-7.
6. Nestle FO, Kaplan DH, Barker J. Psoriasis. New England Journal of Medicine. 2009 Jul;361(5):496–509. Available from: https://doi.org/10.1056/NEJMra0804595.
7. Gudjonsson JE, Elder JT. Psoriasis. In: Kang S, Amagai M, Bruckner AL, editors. Fitzpatrick's Dermatology. 9th ed. McGraw-Hill Education; 2019. p. 456–497.
8. Rizzo HL, Kagami S, Phillips KG, Kurtz SE, Jacques SL, Blauvelt A. IL-23–Mediated Psoriasis-Like Epidermal Hyperplasia Is Dependent on IL-17A. The Journal of Immunology. 2011;186(3):1495–1502. Available from: https://doi.org/10.4049/jimmunol.1001001.
9. Gaffen SL, Jain R, Garg AV, Cua DJ. The IL-23–IL-17 immune axis: from mechanisms to therapeutic testing. Nature Reviews Immunology. 2014 Sep;14(9):585–600. Available from: https://doi.org/10.1038/nri3707.
10. Harper EG, Guo C, Rizzo H, et al. Th17 cytokines stimulate CCL20 expression in keratinocytes in vitro and in vivo: implications for psoriasis pathogenesis. Journal of Investigative Dermatology. 2009 Sep;129(9):2175–2183. Available from: https://doi.org/10.1038/jid.2009.65.
11. Toy D, Kugler D, Wolfson M, et al. Cutting Edge: Interleukin 17 Signals through a Heteromeric Receptor Complex. The Journal of Immunology. 2006;177(1):36–39. Available from: https://doi.org/10.4049/jimmunol.177.1.36.
12. Nograles KE, Zaba LC, Guttman-Yassky E, et al. Th17 cytokines interleukin (IL)-17 and IL-22 modulate distinct inflammatory and keratinocyte-response pathways. British Journal of Dermatology. 2008 Nov;159(5):1092–1102. Available from: https://doi.org/10.1111/j.1365-2133.2008.08769.x.
13. Stritesky GL, Yeh N, Kaplan MH. IL-23 promotes maintenance but not commitment to the Th17 lineage. Journal of Immunology. 2008 Nov;181(9):5948–5955. Available from: https://doi.org/10.4049/jimmunol.181.9.5948.
14. Bovenschen HJ, van de Kerkhof PC, van Erp PE, Woestenenk R, Joosten I, Koenen HJ. Foxp3+ regulatory T cells of psoriasis patients easily differentiate into IL-17A-producing cells and are found in lesional skin. Journal of Investigative Dermatology. 2011 Sep;131(9):1853–1860. Available from: https://doi.org/10.1038/jid.2011.139.
15. Yang XP, Ghoreschi K, Steward-Tharp SM, et al. Opposing regulation of the locus encoding IL-17 through direct, reciprocal actions of STAT3 and STAT5. Nature Immunology. 2011 Mar;12(3):247–254. Available from: https://doi.org/10.1038/ni.1995.
16. van der Fits L, Mourits S, Voerman JS, et al. Imiquimod-induced psoriasis-like skin inflammation in mice is mediated via the IL-23/IL-17 axis. Journal of Immunology. 2009 May;182(9):5836–5845. Available from: https://doi.org/10.4049/jimmunol.0802999.
17. Gong B, Zheng L, Lu Z, et al. Mesenchymal stem cells negatively regulate CD4(+) T cell activation in patients with primary Sjögren syndrome through the miRNA-125b and miRNA-155 TCR pathway. Molecular Medicine Reports. 2021 Jan;23(1). Available from: https://doi.org/10.3892/mmr.2020.11681.
18. Sato K, Ozaki K, Oh I, et al. Nitric oxide plays a critical role in suppression of T-cell proliferation by mesenchymal stem cells. Blood. 2007 Jan;109(1):228–234. Available from: https://doi.org/10.1182/blood-2006-02-002246.
19. Lee S, Kim S, Chung H, Moon JH, Kang SJ, Park CG. Mesenchymal stem cell-derived exosomes suppress proliferation of T cells by inducing cell cycle arrest through p27kip1/Cdk2

signaling. Immunology Letters. 2020 Sep;225:16–22. Available from: https://doi.org/10.1016/j.imlet.2020.06.006.
20. Luz-Crawford P, Noël D, Fernandez X, et al. Mesenchymal stem cells repress Th17 molecular program through the PD-1 pathway. PLoS ONE. 2012;7(9):e45272. Available from: https://doi.org/10.1371/journal.pone.0045272.
21. Ghannam S, Pène J, Moquet-Torcy G, Jorgensen C, Yssel H. Mesenchymal stem cells inhibit human Th17 cell differentiation and function and induce a T regulatory cell phenotype. Journal of Immunology. 2010 Jul;185(1):302–312. Available from: https://doi.org/10.4049/jimmunol.0902007.
22. de Witte SFH, Luk F, Sierra Parraga JM, et al. Immunomodulation By Therapeutic Mesenchymal Stromal Cells (MSC) Is Triggered Through Phagocytosis of MSC By Monocytic Cells. Stem Cells. 2018;36(4):602–615. Available from: https://doi.org/10.1002/stem.2779.
23. Manferdini C, Paolella F, Gabusi E, et al. Adipose stromal cells mediated switching of the pro-inflammatory profile of M1-like macrophages is facilitated by PGE2: in vitro evaluation. Osteoarthritis and Cartilage. 2017 Jul;25(7):1161–1171. Available from: https://doi.org/10.1016/j.joca.2017.01.011.
24. Levy O, Kuai R, Siren EMJ, et al. Shattering barriers toward clinically meaningful MSC therapies. Science Advances. 2020 Jul;6(30):eaba6884. Available from: https://doi.org/10.1126/sciadv.aba6884.
25. Wen K, Li W, Cheng C, et al. Human dental pulp stem cells ameliorate the imiquimod-induced psoriasis in mice. Heliyon. 2023 Feb;9(2):e13337. Available from: https://doi.org/10.1016/j.heliyon.2023.e13337.
26. Ye Z, Liang Y, Lin B, et al. Gingiva-Derived Mesenchymal Stem Cells Attenuate Imiquimod- (IMQ-) Induced Murine Psoriasis-Like Skin Inflammation. Stem Cells International. 2022;p. 6544514. Available from: https://doi.org/10.1155/2022/6544514.
27. Prasanna SJ, Gopalakrishnan D, Shankar SR, Vasandan AB. Pro-inflammatory cytokines, IFNgamma and TNFalpha, influence immune properties of human bone marrow and Wharton jelly mesenchymal stem cells differentially. PLoS ONE. 2010 Feb;5(2):e9016. Available from: https://doi.org/10.1371/journal.pone.0009016.
28. Sareen N, Sequiera GL, Chaudhary R, et al. Early passaging of mesenchymal stem cells does not instigate significant modifications in their immunological behavior. Stem Cell Research & Therapy. 2018 May;9(1):121. Available from: https://doi.org/10.1186/s13287-018-0867-4.
29. Dominici M, Le Blanc K, Mueller I, et al. Minimal criteria for defining multipotent mesenchymal stromal cells. The International Society for Cellular Therapy position statement. Cytotherapy. 2006;8(4):315–317. Available from: https://doi.org/10.1080/14653240600855905.
30. Li Q, Liu W, Gao S, Mao Y, Xin Y. Application of imiquimod-induced murine psoriasis model in evaluating interleukin-17A antagonist. BMC Immunology. 2021 Jan;22(1):11. Available from: https://doi.org/10.1186/s12865-021-00401-3.
31. Chen WC, Wen CH, Wang M, et al. IL-23/IL-17 immune axis mediates the imiquimod-induced psoriatic inflammation by activating ACT1/TRAF6/TAK1/NF-κB pathway in macrophages and keratinocytes. Kaohsiung Journal of Medical Sciences. 2023 Aug;39(8):789–800. Available from: https://doi.org/10.1002/kjm2.12683.
32. Yanping H, Ting G, Xinzhu Z, et al. Yinxie I Formula attenuates imiquimod-induced psoriasis-like skin inflammation via IL-23/IL-17 axis. Archives of Dermatological Research. 2024 Aug;316(8):540. Available from: https://doi.org/10.1007/s00403-024-03288-3.
33. Liu J, Ding Y, Liu Z, Liang X. Senescence in Mesenchymal Stem Cells: Functional Alterations, Molecular Mechanisms, and Rejuvenation Strategies. Frontiers in Cell and Developmental Biology. 2020;8:258. Available from: https://doi.org/10.3389/fcell.2020.00258.
34. Wiese DM, Ruttan CC, Wood CA, Ford BN, Braid LR. Accumulating Transcriptome Drift Precedes Cell Aging in Human Umbilical Cord-Derived Mesenchymal Stromal Cells Serially Cultured to Replicative Senescence. Stem Cells Translational Medicine. 2019 Sep;8(9):945–958. Available from: https://doi.org/10.1002/sctm.18-0246.
35. Seo Y, Kim HS, Hong IS. Stem Cell-Derived Extracellular Vesicles as Immunomodulatory Therapeutics. Stem Cells International. 2019;p. 5126156. Available from: https://doi.org/10.1155/2019/5126156.
36. Bruno S, Deregibus MC, Camussi G. The secretome of mesenchymal stromal cells: Role of extracellular vesicles in immunomodulation. Immunology Letters. 2015 Dec;168(2):154–158. Available from: https://doi.org/10.1016/j.imlet.2015.06.007.
37. Cheng A, Choi D, Lora M, Shum-Tim D, Rak J, Colmegna I. Human multipotent mesenchymal stromal cells cytokine priming promotes RAB27B-regulated secretion of small extracellular vesicles with immunomodulatory cargo. Stem Cell Research & Therapy. 2020 Dec;11(1):539. Available from: https://doi.org/10.1186/s13287-020-02050-6.
38. Song N, Scholtemeijer M, Shah K. Mesenchymal Stem Cell Immunomodulation: Mechanisms and Therapeutic Potential. Trends in Pharmacological Sciences. 2020 Sep;41(9):653–664. Available from: https://doi.org/10.1016/j.tips.2020.06.009.
39. Cui L, Chen R, Subedi S, et al. Efficacy and safety of biologics targeting IL-17 and IL-23 in the treatment of moderate-to-severe plaque psoriasis: A systematic review and meta-analysis of randomized controlled trials. International Immunopharmacology. 2018 Sep;62:46–58. Available from: https://doi.org/10.1016/j.intimp.2018.06.020.
40. Sawyer LM, Malottki K, Sabry-Grant C, et al. Assessing the relative efficacy of interleukin-17 and interleukin-23 targeted treatments for moderate-to-severe plaque psoriasis: A systematic review and network meta-analysis of PASI response. PLoS ONE. 2019;14(8):e0220868. Available from: https://doi.org/10.1371/journal.pone.0220868.